An Energy Formulation for Preisach Models

Ralph C. Smith * and Stefan Seelecke †

*Center for Research in Scientific Computation, North Carolina State Univ., Raleigh, NC 27695
†Mechanical and Aerospace Engineering, North Carolina State University, Raleigh, NC 27695

Abstract

Preisach models formulated in terms of density or measure-based expansions have proven highly successful for characterizing hysteresis and constitutive nonlinearities in materials where the underlying physics is difficult to quantify. This provides a rich mathematical framework for characterizing nonlinear material behavior as well as a framework which facilitates either full or approximate inversion for linear control design. However, the lack of an energy basis for Preisach representations yields models which often have a large number of parameters and are difficult to update to accommodate changing operating conditions (e.g., temperature) since the model parameters are not correlated with physical quantities. Moreover, it is difficult in general to incorporate the frequency-dependence exhibited by essentially all smart materials without resorting to vector-valued parameters or measures which much be identified throughout the range of operation for the system. In this paper, we develop an energy formulation for Preisach models through consideration of appropriate Gibbs and Helmholtz free energy representations. This permits the incorporation of frequency and temperature-dependence in the underlying basis, rather than in parameters identified for a specific system which expands significantly the flexibility of the technique.

Keywords: Preisach model, free energy model, hysteresis, constitutive nonlinearities

1. Introduction

Essentially all currently employed smart materials exhibit some degree of hysteresis in the relation between input fields, temperatures, or stresses, and output displacements. While the severity of hysteresis can be mitigated in many operating regimes through feedback mechanisms or judicious choice of drive electronics, it is necessary to quantify the hysteresis in a manner conducive to control design to achieve the full capabilities of piezoelectric, magnetostrictive and shape memory compounds in smart transducer designs.

One technique for characterizing hysteresis in these materials is through Preisach models based on elemental hysteresis kernels. An advantage of this approach lies in the rich mathematical framework which it provides along with its capability for general material characterization including guaranteed closure of minor loops. Due to its mathematical basis, Preisach theory can be readily applied to regimes in which the underlying physics is difficult to quantify or poorly understood. However, the generality of the method also precludes the incorporation of known physics and can produce models having a large number of nonphysical parameters. Moreover, it is difficult to incorporate the frequency and temperature-dependence exhibited by essentially all smart materials without resorting to vector-valued measures, or parameters, which must be identified throughout the full operating range of the transducer.

In this paper, we develop an energy formulation for Preisach models based on free energy representations for the dipole switching or phase transitions exhibited by the materials in combination with statistical distributions which incorporate effects due to lattice nonuniformities, polycrystallinity, and effective field variations. This

*Email: rsmith@eos.ncsu.edu; Telephone: 919-515-7552
†Email: stefan_seelecke@ncsu.edu; Telephone: 919-515-5282

provides a basis which, at fixed temperatures, frequencies, or loads, can be identified with current Preisach bases or hysterons. For variable conditions, however, the temperature, frequency or load dependence is incorporated in the energy basis rather than the parameters as is the case with classical Preisach formulations. This eliminates the necessity of vector-valued parameters or lookup tables for broadband operation or conditions in which the temperature or load exhibit significant variation. Furthermore, the consideration of an energy derivation of the hysteresis kernels provides physical interpretations for a number of the parameters and reduces significantly the number of parameters required to characterize asymmetric hysteresis loops. These properties augment the efficiency of the model.

We will focus primarily on hysteresis models for piezoceramic materials to simplify the exposition. The main conclusions can be directly extended, however, to magnetostrictive and shape memory compounds due to the universality of the models. In Section 2, we summarize the development of current Preisach models, and the energy formulation for the models is derived in Section 3. Certain properties of the models are illustrated through examples in Section 4.

2. Preisach Models

Preisach models provide a very general methodology for characterizing hysteresis in essentially any materials by quantifying the phenomenon in terms of Preisach kernels with measures, or densities, which are identified for the specific application under consideration. To simplify the discussion, we will focus on the development of Preisach models for piezoceramic materials while noting that analogous models have been employed for magnetic and magnetostrictive materials as well as shape memory compounds. The reader is referred to [6, 8, 16] for discussion regarding the construction of Preisach models for piezoceramic materials and [1, 9, 13] for details about analogous models for shape memory alloys. The classical Preisach theory was developed for characterizing hysteresis in magnetic compounds [15] and overviews in this context can be found in [5, 12]. The formulation and implementation of Preisach models, along with approximate inverse compensator techniques, for control design is addressed in [21]. Due to the maturity of Preisach theory, these citations should be considered as a representative, but not complete, set of references on the subject.

Preisach's original formulation [15] modeled hysteresis in the relation between input magnetic fields $v(t)$ and the magnetization $M(t)$ through a superposition of hysteresis relays or kernels $[k_{s_1,s_2}(v)](t)$ of the form depicted in Figure 1a. Here s_1 and s_2, with $s_1 < s_2$, provide thresholds at which the kernel switches between $+1$ and -1. The magnetization is modeled as

$$M(t) = [P(v)](t) = \int_0^\infty \int_{-\infty}^\infty w(r,s)[k_{s-r,s+r}(v)](t)dsdr \tag{1}$$

where w is a density, or weighting, function which depends on properties of the material under consideration [3]. For typical applications, w is assumed to decay for large s and r which permits truncation of the domain to compact regions.

The magnetic model (1) has been subsequently extended to the formulation

$$[P_w(v,\xi)](t) = \int_{\overline{S}} w(s_1,s_2)[k_s(v,\xi)](t)ds \tag{2}$$

on the closed Preisach plane $\overline{S} = \{(s_1,s_2) \,|\, s_1 \le s_2\}$, as depicted in Figure 2, for arbitrary inputs v and initial states ξ. While the formulation (2) is commonly employed for quantifying hysteresis in a wide variety of materials, it does not provide a framework suitable for establishing the convergence of common approximation schemes [1] or extension to related models including that of Prantl. These latter criteria are provided by the more general formulation

$$[P_\mu(v,\xi)](t) = \int_{\overline{S}} [k_s(v,\xi(s))](t)\, d\mu(s) \tag{3}$$

where $\mu \in \mathcal{M}$ is a finite signed Borel measure on $\overline{S}$. In this case, the measure must be identified for a given choice of kernel k_s and set of operating conditions. We now consider three techniques for constructing k_s.

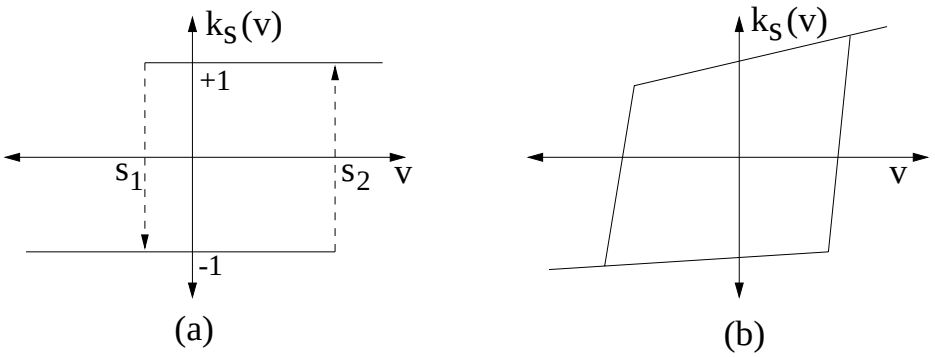

Figure 1. (a) Classical Preisach relay with threshold values s_1 and s_2; (b) Piecewise linear hysteresis kernel employed in [22].

A commonly employed choice for the kernel is the multivalued relay operator depicted in Figure 1a. This kernel can be defined as

$$[k_s(v,\xi)](t) = \begin{cases} [k_s(v,\xi)](0) & \text{if} \quad \tau(t) = \emptyset \\ -1 & \text{if} \quad \tau(t) \neq \emptyset \text{ and } v(\max \tau(t)) = s_1 \\ +1 & \text{if} \quad \tau(t) \neq \emptyset \text{ and } v(\max \tau(t)) = s_2 \end{cases}$$

where the crossing terms τ are defined by

$$\tau(t) = \{\eta \in (0,T] \,|\, u(\eta) = s_1 \text{ or } u(\eta) = s_2\}\,.$$

The starting value

$$[k_s(v,\xi)](0) = \begin{cases} -1 & \text{if} \quad v(0) \leq s_1 \\ \xi & \text{if} \quad s_1 < v(0) < s_2 \\ +1 & \text{if} \quad v(0) \geq s_2 \end{cases}$$

defines the initial state of the kernel in terms of the parameter $\xi \in \{-1, 1\}$.

While this provides an operator which is useful for many applications, this classical definition does not yield a kernel, and hence operator, which is continuous with respect to either time or parameters. Specifically, as proven in [1], the mapping in time

$$t \mapsto [k_s(v,\xi)](t)$$

and the parameter space mapping

$$s \mapsto [k_s(v,\xi)](t)$$

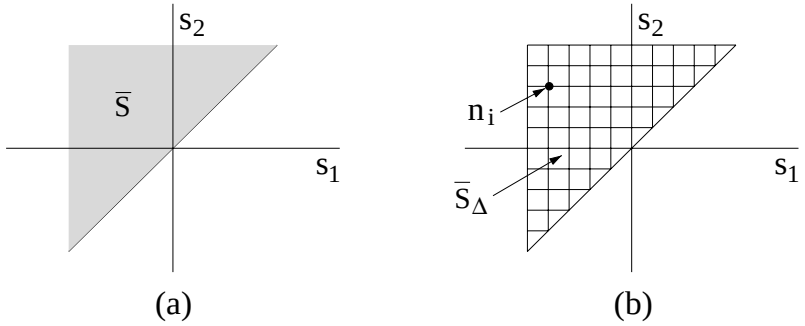

Figure 2. (a) Preisach plane $\overline{S}$; (b) Restricted Preisach plane $\overline{S}_\Delta$.

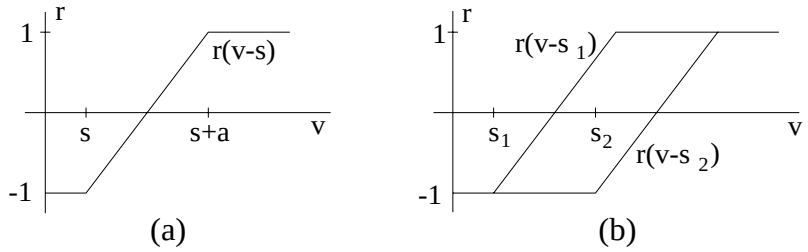

Figure 3. (a) Ridge function $r(v-s)$; (b) Hysteresis envelop provided by the translates r_1 and r_2 of the ridge function $r(v)$.

are discontinuous for the classical Preisach kernel $k_s(v,\xi)$. Continuity in time is important from a physical perspective while continuous parameter dependence is crucial for the development of practical parameter estimation methods.

To avoid the difficulties associated with discontinuous mappings and to provide additional kernels amenable to inversion for control design, we mention two other choices which have been considered for characterizing hysteresis in smart systems. The first is the piecewise linear kernel depicted in Figure 1b. As detailed in [22], this choice proves advantageous in adaptive control design due to its simplicity in combination with its linear dependence on parameters. The second choice is the Krasnolselskii-Pokrovskii (KP) operator.

To define the KP kernel, we consider translates $r_{s_1} = r(v-s_1)$ and $r_{s_2} = r(v-s_2)$ of a Lipschitz continuous ridge function $r(v)$ as depicted in Figure 3. For time intervals $[t_{k-1}, t_k]$ where the input v is monotone, a monotone operator is recursively defined by

$$[\mathcal{R}(v,\mathcal{R}_{k-1})](t) = \begin{cases} \max\{\mathcal{R}_{k-1}, r(v(t)-s_2)\} & \text{if } v \text{ is non-decreasing} \\ \min\{\mathcal{R}_{k-1}, r(v(t)-s_1)\} & \text{if } v \text{ is non-increasing} \end{cases}$$

where

$$\mathcal{R}_k = \begin{cases} \mathcal{R}(v,\mathcal{R}_{k-1})(t_k)\ , & k = 2,\cdots,j \\ \mathcal{R}_0 = \xi\ , & k = 1, \xi \in \{-1,1\} \end{cases}$$

defines the values of $\mathcal{R}$ at times t_k. The KP kernel is then defined recursively on each subinterval by

$$[k_s(v,\xi)](t) = [\mathcal{R}(v,\mathcal{R}_{k-1})](t) \quad , \quad t \in [t_{k-1}, t_k]\,.$$

A typical path for k_s is depicted in Figure 4 while details concerning the properties of the kernel are provided in [1, 2].

To numerically implement the model, the measure $\mu(s)$ is approximated by the expansion

$$\mu_m = \sum_{i=1}^{m} \alpha_{n_i} \delta_{n_i}$$

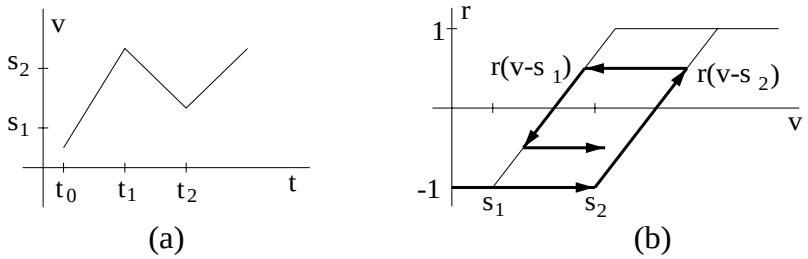

Figure 4. (a) Piecewise monotone input $v(t)$; (b) Output from the KP kernel in response to the input.

where, as depicted in Figure 2b, n_i are nodes in the restricted Preisach plane $\overline{S}_\Delta = \{(s_1, s_2) \,|s_{min} \leq s_1 \leq s_2 \leq s_{max}\}$, α_{n_i} are weights, and δ_{n_i} denotes the Dirac measure having an atom at n_i. The KP operator P_μ is then approximated by P_m given by

$$[P_m(v,\xi)](t) = \sum_{i=1}^{m} [k_{n_i}(v, \xi_{n_i})](t)\alpha_{n_i} \, .$$

As detailed in [1, 2, 7], the continuity and convergence properties of the KP operator lead to well-posedness of the corresponding identification problem and provide a framework which is amenable to implementation.

A number of difficulties associated with Preisach models complement the previously mentioned advantages. First, the nonphysical nature of the measures or parameters makes it difficult to construct models using known physical behavior or to employ attributes of the data for updating models to accommodate changing operating conditions. Furthermore, a large number of parameters can be required to accurately characterize asymmetric, biased hysteresis loops.

A more fundamental difficulty arises in operating regimes involving broadband input signals and temperature or load-dependence in the hysteresis. All smart materials exhibit some degree of frequency, temperature and load dependence in their measured hysteresis loops whereas classical Preisach models are based on the assumption of frequency, temperature and load invariance [3]. While extensions to the classical theory have been been developed to address these difficulties (e.g., see [5] for discussion of modifications to accommodate dynamic effects in magnetic materials), they add significantly to the complexity of the method.

To illustrate, consider the approach employed by Krejčí and Sprekels [10] to incorporate temperature dependence in a general hysteresis operator through vector-valued measures. Rather than employ the general relation (3), one would instead define the Preisach operator to be

$$[P_\mu(v,\xi;\theta)](t) = \int_{\overline{S}} [k_s(v,\xi(s))](t)\, d\mu_\theta(s) \tag{4}$$

where $\mu_\theta(s)$ is a vector-valued measure. This extension, as well as analogous extensions to incorporate load or frequency dependence, makes the method significantly more difficult to implement for either material characterization or control design.

Additional modifications to the classical theory must be made to accommodate reversible changes in polarization or magnetization measured at low drive levels or to relax congruency requirements to ensure that minor loops remain inside major loops (see [5, 11] for discussion regarding these extensions for magnetic materials). In combination, these difficulties motivate the definition of Preisach kernels based on energy formulations for the problem.

3. Free Energy Formulation

To construct an energy-based hysteresis kernel, we consider first the energy required to reorient dipoles in a single crystal ferroelectric material assumed initially to have uniform lattice spacing. The effects of nonuniform lattice points, polycrystallinity and variations in effective fields are incorporated through the introduction of various distributions. It is then illustrated that these distributions provide the measures or densities employed in the classical Preisach formulation. We focus on ferroelectric materials to simplify the discussion but note that because the theory summarized here is an extension of the Müller-Achenbach-Seelecke theory for shape memory alloys [14, 17], similar conclusions can be made for SMA compounds.

In addition to providing an energy basis for Preisach kernels, it will be established that development of a model in this manner places the temperature, frequency and load dependence in the hysteresis basis or kernel rather than in the parameters as indicated in (4). This greatly facilitates the implementation of the model for broadband applications or slowly varying operating conditions.

As detailed in [20], the first step in the development of a free energy model for piezoceramic materials is based on the assumption that dipoles in a single crystal with uniform lattice spacing can have two orientations, which we denote by $s_1 = 1$ and $s_{-1} = -1$, due to the proclivity for Ti^{4+} ions to attain equilibrium positions which minimize the free energy (see Figure 5). This yields an energy landscape of the form depicted in Figure 6.

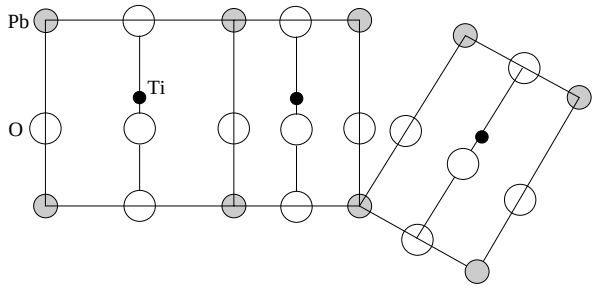

Figure 5. Nonuniform lattice and polycrystalline structure for PZT.

The application of a field E distorts the landscape causing dipoles to switch when local minima disappear. The goal in this component of the model development is to quantify the energy and resulting relation between the field and polarization to provide a means of specifying the hysteresis kernel k_s. This discussion summarizes the model developed in [20] and the reader is referred to that source for details.

For the uniform lattice, an appropriate form of Gibbs free energy is

$$G = \psi - EP$$

where ψ denotes the Helmholtz free energy density. One choice for ψ, based on statistical mechanics, is

$$\psi(P,T) = \frac{\Phi_0 N}{4V}[1-(P/P_s)^2] + \frac{TkN}{2VP_s}\left[P\ln\left(\frac{P+P_s}{P_s-P}\right) + P_s\ln(1-(P/P_s)^2)\right]$$

where Φ_0 is the energy required to convert the orientation at a single site, N is the number cells in the volume V having dipole moment p_0, and $P_s = Np_0/V$ is the saturation polarization. For fixed temperatures, a second choice for ϕ is

$$\psi(P) = \begin{cases} \frac{1}{2}E_1(P+P_T)^2 & , \ P \le -P_1 \\ \frac{1}{2}E_1(P-P_T)^2 & , \ P \ge P_1 \\ \frac{1}{2}E_1(P_1-P_T)\left[\frac{P^2}{P_1}-P_T\right] & , |P| < P_1 \end{cases}$$

where P_T, P_1 and E_1 are related to physical properties of the data.

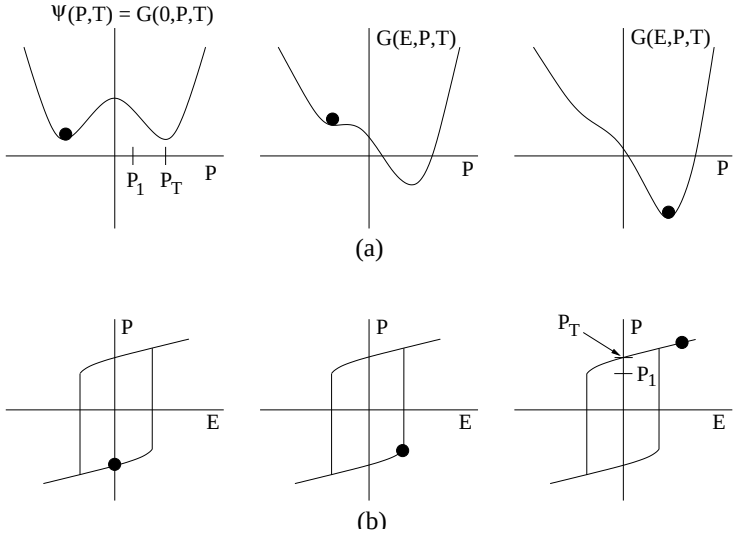

Figure 6. (a) Helmholtz energy ψ and Gibbs energy G for increasing field E; (b) Polarization P as a function of E for a single crystal with uniform lattice.

To model the polarization generated by a given field, Boltzmann principles are invoked to quantify the probability

$$\mu(G) = Ce^{-G/kT}$$

of finding dipoles with free energy G. Here k denotes Boltzmann's constant. The average polarizations due to dipoles having positive and negative orientation are then respectively given by

$$\langle P_+ \rangle = \frac{\int_{P_1}^{\infty} Pe^{-G(E,P,T)V/kT} dP}{\int_{P_1}^{\infty} e^{-G(E,P,T)V/kT} dP}$$

$$\langle P_- \rangle = \frac{\int_{-\infty}^{-P_1} Pe^{-G(E,P,T)V/kT} dP}{\int_{-\infty}^{-P_1} e^{-G(E,P,T)V/kT} dP}$$

and the average polarization for the lattice volume is

$$\overline{P} = x_+ \langle P_+ \rangle + x_- \langle P_- \rangle \ . \tag{5}$$

The dipole fractions satisfy the differential equations

$$\dot{x}_+ = -p_{+-}x_+ + p_{-+}x_-$$
$$\dot{x}_- = -p_{-+}x_- + p_{+-}x_+$$

which can be simplified to

$$\dot{x}_+ = -p_{+-}x_+ + p_{-+}(1 - x_+)$$

through the identity $x_+ + x_- = 1$. Finally, we note that the likelihoods of a dipole switching from $+$ to $-$, and alternatively from $-$ to $+$, are given by

$$p_{+-} = \sqrt{\frac{kT}{2\pi m}} \frac{e^{-G(E,P_1(T),T)V/kT}}{\int_{P_1}^{\infty} e^{-G(E,P,T)V/kT} dP}$$

$$p_{-+} = \sqrt{\frac{kT}{2\pi m}} \frac{e^{-G(E,-P_1(T),T)V/kT}}{\int_{-\infty}^{-P_1} e^{-G(E,P,T)V/kT} dP} .$$

The contribution $g(\omega) = \sqrt{\frac{kT}{2\pi m}}$, where m denotes the mass of the lattice volume, incorporates the dynamic effects due to the mean speed of fluctuations in the polarization.

The solution of (5) specifies the hysteresis relation between E and P over a lattice volume as depicted in Figure 6. Hence this comprises a fundamental hysteresis kernel k_s employed in the Preisach formulations summarized in Section 2. Specifically, if we let $v = E$ denote the input and ξ the initial dipole state, then the kernel elements can be defined as

$$[k_s(v, \xi, T, \omega)](t) = [\overline{P}(v, \xi, T, \omega)](t).$$

We point out that while the kernels depicted in Figure 6 appear similar to those described in Section 2, these energy-based kernels incorporate the temperature and potential load dependence constructed in the free energy expressions and the frequency-dependence incorporated in the transition probabilities. Through the energy derivation, these effects are thus incorporated in the basis rather than the parameters as was the case for the classical Preisach model.

To extend the model from uniform lattice volumes to polycrystalline materials having nonuniform lattices and effective field variations, we consider distributions of certain input parameters and fields. To incorporate variations in the lattice structure, we consider the lattice parameter $\widetilde{E}_1 = E_1(P_T - P_1)$ to be normally distributed; that is we assume that it has the density

$$f(\widetilde{E}_1) = C_1 e^{-(\widetilde{E}_1 - \bar{E}_1)^2/b}$$

where $\bar{E}_1$ denotes a mean coercive field at which dipoles switch. Effective field effects (see [18, 19]) are incorporated by assuming that the actual field at the domain level has the density

$$\widehat{f}(\mathcal{E}) = C_2 e^{-(\mathcal{E}-E)^2/\bar{b}}$$

where E denotes the applied field. The combined polarization model is then

$$[P(E,\omega,T)](t) = C \int_0^\infty \int_{-\infty}^\infty [\overline{P}(\mathcal{E}+E, \widetilde{E}_1, \omega, T)](t) e^{-\mathcal{E}^2/\bar{b}} e^{-(\widetilde{E}_1 - \bar{E}_1)^2/b} d\mathcal{E} d\widetilde{E}_1 \,. \tag{6}$$

It is observed that the hysteresis operator defined by (6) has the form (1) with the density function defined by

$$w(\mathcal{E}, \widetilde{E}_1) = C e^{-\mathcal{E}^2/\bar{b}} e^{-(\widetilde{E}_1 - \bar{E}_1)^2/b}. \tag{7}$$

We note that a number of authors have employed analogous Gaussian densities in classical Preisach models, modified to incorporate interaction fields, when characterizing hysteresis in magnetic materials [5, 11]. In contrast to the classical model, however, the energy kernel $k_s = \overline{P}$ incorporates temperature effects in addition to certain dynamic properties. This alleviates the difficulty associated with incorporating these dependencies in the density or parameters of classical Preisach models.

4. Numerical Example

To illustrate certain capabilities of the model, we consider the numerical simulation of symmetric major and minor loops as well as biased, asymmetric minor loops. To remain consistent with the derivation, the example is considered in the context of characterizing the hysteretic relation between input electric fields and the polarization in piezoelectric materials.

For the simulations, the parameters were taken to be $E_1 = 7 \times 10^8, P_T = 0.0285, \bar{E} = 4 \times 10^6, b = 4.5 \times 10^{11}$, $\bar{b} = 3 \times 10^4$ and $C = 9.5 \times 10^{-12}$. As illustrated in [20], these parameter values are commensurate with values obtained when validating the model through comparison with experimental data.

The field plotted in Figure 7a was provided as input to the model to simulate the response of the material to biased and unbiased field oscillations. The resulting polarization is plotted as a function of the input field in Figure 7b. Loop 1 illustrates the capability of the model to characterize the quadratic Raleigh behavior experimentally observed for low input levels whereas Loops 2, 3 and 4 illustrate that the model enforces closure of biased, asymmetric minor loops. The continuity in slope of the initial polarization curve, following the closure of Loop 2, also illustrates that the model incorporates the 'wiping out property' which, along with congruency, forms one of the necessary and sufficient conditions for classical Preisach models [12]. Finally, Loop 5 illustrates that the model characterizes the saturation behavior present at high drive levels. When combined with the experimental results summarized in [20], the behavior summarized here provides the model with substantial flexibility for material characterization and control design.

5. Concluding Remarks

This paper summarizes an energy formulation for Preisach models used to quantify the hysteresis and constitutive nonlinearities inherent to various smart materials. In the first step of the development, free energy relations quantifying the average polarization at the lattice level were derived and used to construct fundamental

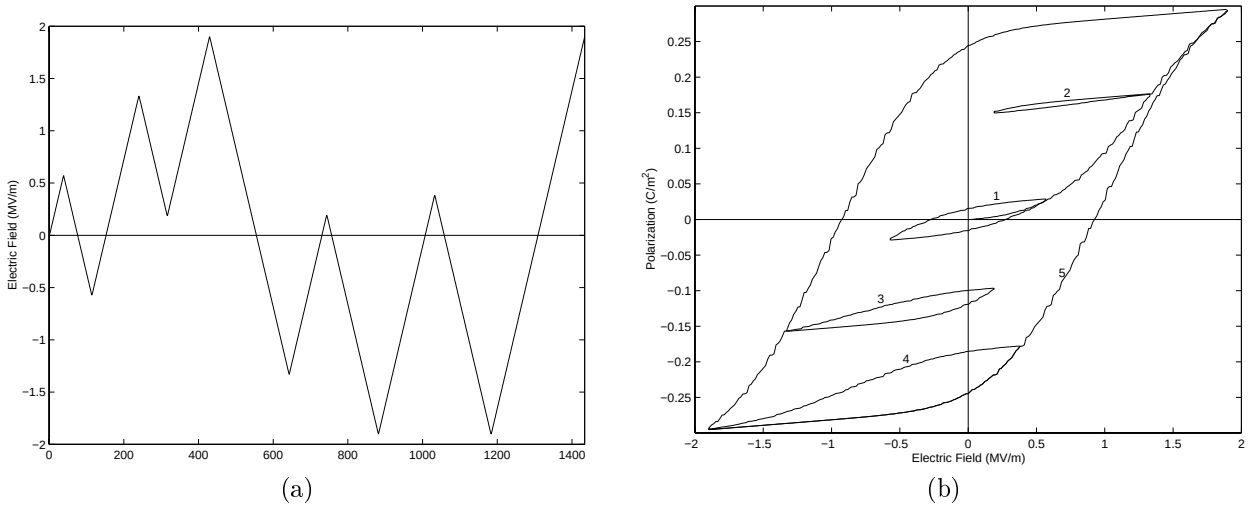

(a) (b)

Figure 7. (a) Input field E to the model; (b) Polarization predicted by the model.

hysteresis kernels or basis elements. These kernels are analogous to the relays employed in Preisach models with the following exception; the kernels in Preisach models are formulated under the assumption of frequency and temperature invariance whereas the energy-based kernel incorporates certain temperature and frequency effects through the construction of the free energy functionals. This facilitates construction of the kernels and implementation of the method. In the second step of the development, densities quantifying variations in the effective field and lattice structure were incorporated to provide a macroscopic model for polycrystalline materials. These densities are physical manifestations of the measures or parameters employed in classical Preisach models. The capability of the model to provide minor loop closure and enforce the 'wiping out property' was illustrated through a numerical example while experimental validation of the model is provided in [20].

Acknowledgements

The research of R.C.S. was supported in part through the NASA grant NAG-1-01041 and in part by the Air Force Office of Scientific Research under the grant AFOSR-F49620-01-1-0107. The research of S.S. was supported in part by the National Science Foundation through the grant DMI-0134464.

References

[1] H.T. Banks, A.J. Kurdila and G. Webb, "Identification of hysteretic control influence operators representing smart actuators Part I: Formulation," *Mathematical Problems in Engineering*, 3 pp. 287-328, 1997.

[2] H.T. Banks, A.J. Kurdila and G. Webb, "Identification of hysteretic control influence operators representing smart actuators Part II: Convergent approximations," *Journal of Intelligent Material Systems and Structures*, 8(6), pp. 536-550, 1997.

[3] M. Brokate and J. Sprekels, *Hysteresis and Phase Transitions*, Springer-Verlag, New York, 1996.

[4] E. Della Torre and F. Vajda, "Parameter identification of the complete moving hysteresis model using major loop data," *IEEE Transactions on Magnetics*, 30(6), 1994.

[5] E. Della Torre, *Magnetic Hysteresis*, IEEE Press, New York, 1999.

[6] W.S. Galinaitis and R.C. Rogers, "Compensation for hysteresis using bivariate Preisach Models," SPIE Smart Structures and Materials, 1997, Mathematics and Control in Smart Structures, San Diego, CA, 1997.

[7] W.S. Galinaitis and R.C. Rogers, "Control of a hysteretic actuator using inverse hysteresis compensation," SPIE Smart Structures and Materials, Mathematics and Control in Smart Structures, San Diego, CA, 1998.

[8] P. Ge and M. Jouaneh, "Modeling hysteresis in piezoceramic actuators," *Precision Engineering*, 17, pp. 211-221, 1995.

[9] Y. Huo, "A mathematical model for the hysteresis in shape memory alloys," *Cont Mech Thermodyn,* 1, pp. 283-303, 1989.

[10] P. Krejčí and J. Sprekels, "On a system of nonlinear PDEs with temperature-dependent hysteresis in one-dimensional thermoplasticity," *Journal of Mathematical Analysis and Applications,* 209, pp. 25-46, 1997.

[11] F. Liorzou, B. Phelps and D.L. Atherton, "Macroscopic models of magnetization," *IEEE Transactions on Magnetics*, 36(2), pp. 418-428, 2000.

[12] I.D. Mayergoyz, *Mathematical Models of Hysteresis,* Springer-Verlag, New York, 1991.

[13] J. Ortin, "Preisach modeling of hysteresis for a pseudoelastic cu-zn-al single crystal," *J Appl Phys*, 71, pp. 1454-1461, 1992.

[14] N. Papenfuß and S. Seelecke, "Simulation and control of SMA Actuators," SPIE Smart Structures and Materials, Mathematics and Control in Smart Structures, San Diego, CA, pp. 586-595, 1999.

[15] F. Preisach, "Uber die magnetische nachwirkung," *Zeitschrift fur Physik*, 94, pp. 277-302, 1935.

[16] G. Robert, D. Damjanovic and N. Setter, "Preisach modeling of piezoelectric nonlinearity in ferroelectric ceramics," *Journal of Applied Physics*, 89(9), pp. 5067-5074, 2001.

[17] S. Seelecke and C. Büskens, "Optimal control of beam structures by shape memory wires," *Computer Aided Optimum Design of Structures,* V.S. Hernández and C.A. Brebbia (Eds.,) Computational Mechanics Publications, pp. 457-466, 1997.

[18] R.C. Smith and C.L. Hom, "Domain wall theory for ferroelectric hysteresis," *Journal of Intelligent Material Systems and Structures*, 10(3), pp. 195-213, 1999.

[19] R.C. Smith and Z. Ounaies, "A domain wall model for hysteresis in piezoelectric materials," *Journal of Intelligent Material Systems and Structures*, 11(1), pp. 62-79, 2000.

[20] R.C. Smith, S. Seelecke and Z. Ounaies, "A free-energy model for piezoceramic materials," Smart Structures and Materials 2002, Modeling, Signal Processing and Control in Smart Structures, to appear.

[21] X. Tan, R. Venkataraman and P.S. Krishnaprasad, "Control of hysteresis: Theory and experimental results," Smart Structures and Materials 2001, Modeling, Signal Processing and Control in Smart Structures, SPIE Vol. 4326, pp. 101-112, 2001.

[22] G. Tao and P.V. Kokotović, *Adaptive Control of Systems with Actuator and Sensor Nonlinearities*, John Wiley and Sons, New York, 1996.